Evaluation of a vortex-based subgrid stress model using DNS databases

By Ashish Misra[1] AND Thomas S. Lund[2]

The performance of a subgrid stress (SGS) model for large-eddy simulation (LES) developed by Misra & Pullin (1996) is studied for forced and decaying isotropic turbulence on a 32^3 grid. The physical viability of the model assumptions are tested using DNS databases. The results from LES of forced turbulence at Taylor Reynolds number $R_\lambda \simeq 90$ are compared with filtered DNS fields. Probability density functions (pdfs) of the subgrid energy transfer, total dissipation, and the stretch of the subgrid vorticity by the resolved velocity-gradient tensor show reasonable agreement with the DNS data. The model is also tested in LES of decaying isotropic turbulence where it correctly predicts the decay rate and energy spectra measured by Comte-Bellot & Corrsin (1971).

1. Introduction

The aim of this study is to use DNS data of isotropic turbulence to evaluate the performance of a new subgrid-stress model. LES is performed for both forced and decaying turbulence, and statistics are compared with appropriately filtered DNS fields and with some experimental results. The SGS stresses are calculated from a structural model of the subgrid vorticity proposed by Pullin & Saffman (1994), henceforth PS. This model has some similarity to the eddy-axis structure model for one-point closure proposed independently by Reynolds & Kassinos (1995). PS assume that the subgrid structure consists of an ensemble of straight stretched vortex structures each with an arbitrary internal vorticity distribution. Some support for this type of structure of the fine scales is provided by the observed tendency, in several numerical simulations, for the alignment between the vorticity vector and the eigenvector corresponding to the algebraically intermediate value of the principal rate-of-strain. Moreover, stretched-vortices have been used to make quantitative predictions for a range of fine-scale turbulence properties (Lundgren 1982, Pullin & Saffman, 1993, 1994). Misra & Pullin (1996) have examined and implemented several different versions of the locally anisotropic model of PS. In this report we will discuss one such model and examine its performance when measured against experiment and filtered DNS.

1 Graduate Aeronautical Laboratory, California Institute of Technology, Pasadena CA 91125

2 Center for Turbulence Research

2. Vortex orientation model

In the PS model, the orientations of the structures are given by a pdf of the distribution of Euler-angles describing the transformation from laboratory to structure-fixed axes. The Reynolds stresses are proportional to the turbulent kinetic energy of the vortex collection times a tensor-moment of the pdf. For example, a delta-function pdf in which all vortices in a subgrid domain have a common direction described by the unit vector $\tilde{\mathbf{e}}$ gives Reynolds stresses,

$$\tau_{ij} = (\delta_{ij} - \tilde{e}_i \tilde{e}_j) \int_{k_c}^{\infty} E(k) dk \tag{1}$$

where k_c is the cutoff wavenumber and the subgrid kinetic energy is given by $K = \int_{k_c}^{\infty} E(k) dk$. PS proposed a simplified version of the model using a rapid-distortion-like approximation in which the orientation of the subgrid vortices have a two-delta function pdf defined by the eigenvectors corresponding to the largest two eigenvalues of the resolved rate-of-strain tensor $\widetilde{S}_{ij}$. It can be shown that such a model can not produce backscatter. In this report we study the performance of a slight variant of their original model wherein there is alignment between the eigenvector corresponding to the maximum eigenvalue of the rate-of-strain tensor, $\tilde{\mathbf{e}}_3$, and the resolved vorticity vector, $\tilde{\omega}$. The Reynolds stresses are then given by

$$T_{ij} = \left(\mu(\delta_{ij} - \tilde{e}_{3i}\tilde{e}_{3j}) + (1-\mu)(\delta_{ij} - e^{\omega}_i e^{\omega}_j)\right) \int_{k_c}^{\infty} E(k) dk, \tag{2}$$

where μ is the fraction of structures aligned with the maximally extensive eigenvector and $\mathbf{e}^{\omega}$ is the unit vector along $\tilde{\omega}$. As partial justification for (2) we remark that one should expect complete alignment with $\tilde{\omega}$ in the DNS limit. We currently take $\mu = 0.5$. In order to calculate the subgrid energy, K, a local balance between production by the resolved scales, and the sum of subgrid and resolved scale dissipation is assumed. When coupled to an assumed Kolmogorov subgrid energy spectrum produced by the (unknown) internal structure of the vortices with a cut-off at $k\eta = 1$, where $\eta = (\nu^3/\epsilon)^{1/4}$ is the local Kolmogorov length, an equation sufficient to determine the dissipation is obtained. This is given by

$$\begin{aligned} \epsilon = 2\nu \widetilde{S}_{ij}\widetilde{S}_{ij} - \frac{3\,K_0}{2\,k_c^{2/3}}\,\epsilon^{2/3}\,\left(1 - (k_c\eta)^{2/3}\right)\,\widetilde{S}_{ij} \\ \times \left(\frac{1}{2}(\delta_{ij} - \tilde{e}_{3i}\tilde{e}_{3j}) + \frac{1}{2}(\delta_{ij} - e^{\omega}_i e^{\omega}_j)\right), \end{aligned} \tag{3}$$

where K_0 is the Kolmogorov constant. When the model parameter K_0 is specified, (3) can be solved for the total dissipation ϵ and the subgrid energy determined from the Kolmogorov spectrum. This gives closure.

Equation (3) has the dimensions of L^2T^{-3}; we therefore divide (3) by $k_c^4\nu^3$ which results in two non-dimensional parameters (see Misra & Pullin for details),

$$\begin{aligned} \hat{S}_1 &= \frac{2\widetilde{S}_{ij}\widetilde{S}_{ij}}{k_c^4\nu^2}, \\ \hat{S}_2 &= \widetilde{S}_{ij}\frac{\left(\frac{1}{2}(\delta_{ij} - \tilde{e}_{3i}\tilde{e}_{3j}) + \frac{1}{2}(\delta_{ij} - e^{\omega}_i e^{\omega}_j)\right)}{2\,k_c^2\nu}, \end{aligned} \tag{4}$$

where $\hat{S}_1$ represents the resolved scale dissipation while $\hat{S}_2$ represents the stretch experienced by the subgrid vortices by the resolved velocity-gradient tensor. The SGS dissipation may be written as,

$$\begin{aligned} \varepsilon_{sgs} &\equiv -\widetilde{S}_{ij}T_{ij}, \\ &= -\widetilde{S}_{ij}\left(\frac{1}{2}(\delta_{ij} - \tilde{e}_{3i}\tilde{e}_{3j}) + \frac{1}{2}(\delta_{ij} - e_i^{\omega}e_j^{\omega})\right) K, \\ &\sim -\widehat{S}_2\, K, \\ &= \tilde{S}'_{str}\, K, \end{aligned} \tag{5}$$

where $\tilde{S}'_{str}$ is the component of $\tilde{S}_{ij}$ aligned with the vortex. Hence backscatter, defined by $\varepsilon_{sgs} < 0$ occurs whenever $\widehat{S}_2 > 0$ - the subgrid vortices are being compressed on the average - while $\widehat{S}_2 < 0$ - the vortices are axially stretched - gives cascade.

This model has been implemented for both forced and decaying box turbulence by Misra & Pullin. They examine several alternative scenarios for determining the instantaneous orientations of vortices in a given cell.

3. Results and discussions

The incompressible, filtered Navier-Stokes equations are solved in a 32^3 box, with and without forcing, using periodic boundary conditions in all three directions. A Fourier-Galerkin pseudo-spectral method is used with '3/2 dealiasing rule' for the non-linear terms, i.e. 32 Fourier modes in each direction were advanced in time, the computation of the non-linear terms were done using 48 modes in each direction. A second order explicit Runge-Kutta scheme is used for time advancement.

3.1 Decaying turbulence

We study decaying isotropic turbulence in order to compare our results to the experiment of Comte-Bellot and Corrsin. They measured the energy spectrum at three downstream locations in grid turbulence. One can relate this to decaying isotropic turbulence by invoking the Taylor approximation. We mimic their experiment by studying turbulence in a cubical box with periodic boundary conditions. In a frame of reference moving with the mean flow speed,

$$t = \int_0^x \frac{dx'}{\overline{U}(x')}$$

where x is the downstream distance from the grid and $\overline{U}(x)$ is the mean flow velocity over the cross-section of the tunnel. We have non-dimensionalized the experimental data by the following characteristic velocity, length and time scales: $U_{ref} = \sqrt{3U_0'^2/2}$, $L_{ref} = L/2\pi$ and $t_{ref} = L_{ref}/U_{ref}$. In their experiments the velocity fluctuation at the first measuring station is $\sqrt{U_0'^2} = 22.2$ cm/s, the free-stream speed is $U_\infty = 10^3$ cm/s and the spacing of the turbulence generating mesh

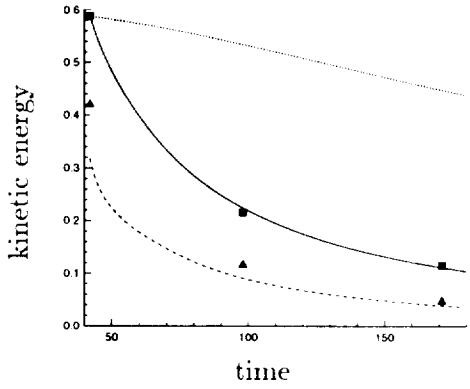

FIGURE 1. Decay of resolved (———) and subgrid (----) kinetic energy. No model: ····· . Experiment: Resolved, ■; subgrid, ▲.

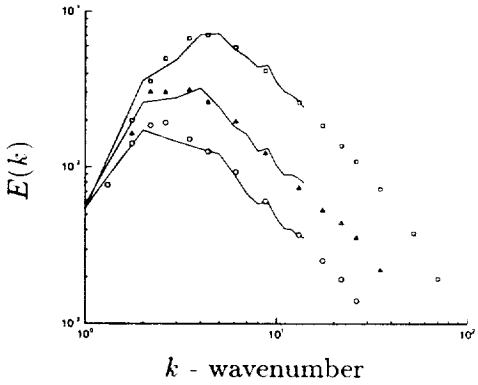

FIGURE 2. Time evolution of spectra in decaying turbulence. Experiment: □ , t=42; △ , t=98; ○ , t=171. Simulation at corresponding times: ——— .

is $M = 5.08$ cm. The size of the computational box, $L = 11M$, was chosen to contain roughly four integral scales. The times at the three stations were measured in terms of $U_\infty t/M$. The initial Taylor Reynolds number is $R_\lambda \simeq 80$. In order to compare the resolved and the subgrid part of the turbulent energy produced by the computation, the measured spectra have been integrated over the relevant scale ranges.

Figure 1 shows the decay of the resolved energy with time. The LES gives good agreement with experiment. The dotted line is the result of running the simulation with the model switched off. It is evident that the model plays an important role in predicting the correct decay of the kinetic energy. Aside from the parameter μ (set to 0.5), the model requires a value of the Kolmogorov constant. While acceptable results were obtained with the standard value of $K_0 = 1.5$, a slight improvement was observed when higher values were used. The results in Fig. 1 were obtained with $K_0 = 1.8$. While this value is on the edge of the uncertainty band from experimental measurements (Sreenivasan 1995), it is well within the predicted range

from numerical simulation; Jiménez *et al.* report a value of $K_0 \approx 2$ in a 256^3 DNS of isotropic turbulence at $R_\lambda = 94.1$. It is possible that elevated values of the Kolmogorov constant in numerical simulations is a low Reynolds number effect. If this is the case, it stands to reason that a larger value should be used in the present simulations which are also performed at relatively low Reynolds number.

The decay of the subgrid energy with time is also shown in Fig. 1. Note that the subgrid energy is obtained from the model without the solution of additional field equations. The subgrid energy is a quantity derived from a knowledge of the resolved field and the chosen subgrid energy spectrum; it therefore can not be initialized to match the experimental value. Figure 2 shows a plot of the resolved energy spectra with the measurements at the initial time and then at the two later instants. The initial spectrum is generated to match the experimental data, while the later two curves are the predicted spectra arising from the LES calculation. Figure 1 gives the area under the curve of Fig. 2 at the three time instants, over the resolved range of scales.

3.2 Forced turbulence

Forcing is achieved by exciting low wavenumbers such that the total energy injection rate is constant in time. A certain selected number of Fourier modes are chosen from a wavenumber shell $|\mathbf{k}| = k_0$. The Fourier coefficient of the forcing term is then written as,

$$\widehat{\mathbf{f}}_k = \frac{\delta}{N} \frac{\widehat{\widehat{\mathbf{U}}}_k^*}{|\widehat{\widehat{\mathbf{U}}}_k|^2} \tag{6}$$

for all modes in the specified shell. The above choice of $\widehat{\mathbf{f}}_k$ ensures that the energy injection rate, $\sum \widehat{\mathbf{f}}_k \cdot \widehat{\widehat{\mathbf{U}}}_k$, is a constant and equal to δ. We have chosen $k_0 = 2, N = 20$, and $\delta = 0.1$ for all the runs. (See Carati *et al.* 1995)

Simulations with forcing were performed such that a statistical steady state is reached when statistics are collected. Results in this report are presented for Taylor Reynolds number, $R_\lambda \simeq 85$ in order to make comparisons with 128^3 DNS results at approximately the same Taylor Reynolds number.

Figure 3a-b shows scatter plots of $\hat{S}_1$ versus $\hat{S}_2$ from the LES as well as from filtered DNS data. These plots show the intensity of the vortex stretch as a function of the resolved dissipation rate. Notice that the DNS data displays a significant fraction of points with positive stretch parameter, $\hat{S}_2$, (backscatter) whereas the model rarely predicts these events. Quantitatively, the DNS shows roughly 30% backscatter, which is consistent with previous measurements (Piomelli *et al.* 1991). In contrast, our model yields only $\sim 3\%$ backscatter. While there is clearly a large discrepancy in the prediction of backscatter in Fig. 3, it should be noted that the percentage of backscatter can be controlled through the parameter μ in Eq. 2. $\mu = 1$ corresponds to complete alignment with $\tilde{\mathbf{e}}_3$ and results in no backscatter, while $\mu = 0$ corresponds to complete alignment with $\tilde{\omega}$ and gives about 40% backscatter. When $0 \leq \mu < 0.4$, the decay of the kinetic energy appears correct, but the decay of the energy spectra is somewhat unsatisfactory with a trend towards flattening of the

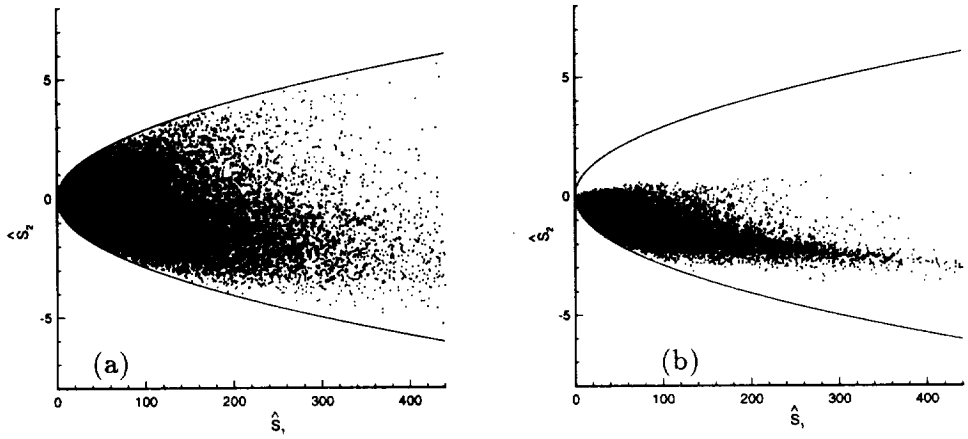

FIGURE 3. Scatter plot of $\hat{S}_1$ and $\hat{S}_2$ in filtered DNS (a) and LES (b).

spectrum at later times. In the range $0.4 \leq \mu \leq 1$, there is a general insensitivity to μ, leading to correct statistics and diminishing backscatter. The performance of the model for all values of μ in forced turbulence is satisfactory. Presently we show results for $\mu = 0.5$ which are typical of the behavior of the decay of the resolved energy spectrum and of the resolved and subgrid energy for $0.4 \leq \mu \leq 1.0$.

An interesting feature of Fig. 3 is that all points lie within a bounding parabola. An estimate based on a locally two-dimensional 'maximum stretch' scenario for $\hat{S}_{ij}$ gives a bounding parabola $\hat{S}_1 = 16\ \hat{S}_2^2$. We find however that $\hat{S}_1 = 12\ \hat{S}_2^2$ gives a slightly better boundary and so this curve is displayed in the figure. The importance of backscatter has been a question of debate though there is some evidence in the literature of its importance in wall-bounded flows. The backscatter property of the model is also illustrated in Fig. 4a, which shows a pdf of the 'stretch', that part of the velocity-gradient tensor which stretches the subgrid vorticity. The stretch is suitably normalized by $\sqrt{\overline{\epsilon}/\nu}$. While the two curves peak at approximately the same location, the LES shows predominant stretching. Figure 4b is a plot of the pdf of the subgrid energy transfer, $\varepsilon_{sgs}/\overline{\epsilon}$; points on the left of the origin exhibit backscatter. It is clear from the figure that the LES does well in the cascade region. The pdf of the total dissipation $\log_{10}(\epsilon/\overline{\epsilon})$ is displayed in Fig. 4c. The total dissipation ϵ is a positive definite quantity by construction as defined in (3). The distribution of ϵ appears to be approximately log-normal.

4. Concluding remarks

The behavior of an SGS model for LES has been tested against filtered DNS fields at similar Reynolds numbers. The model is stable and appears to produce a good quantitative description of the resolved flow and of the subgrid energy. It shows the right decay rate and gives good agreement with the experiments of Comte-Bellot and Corrsin. The model seems to work well for forced turbulence. Misra

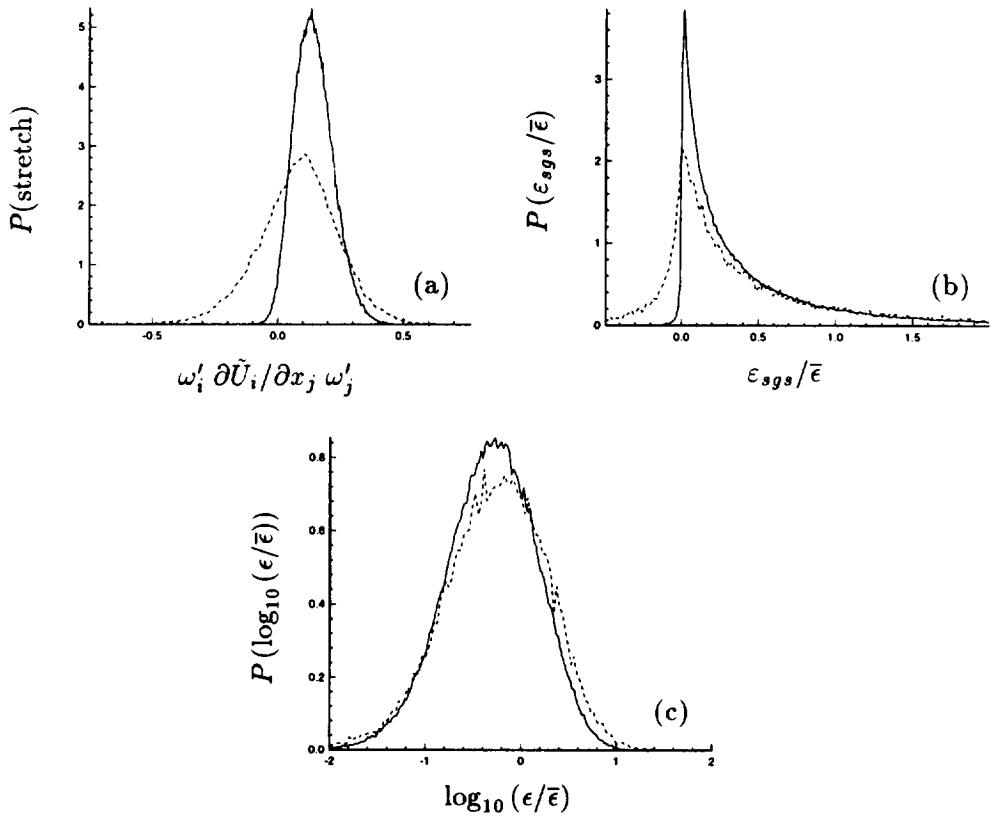

FIGURE 4. Pdf of: (a) stretch, (b) subgrid energy transfer, (c) total dissipation. —— LES, ---- DNS.

& Pullin demonstrate that it produces negligible SGS dissipation in the limit of fully resolved flow. A small amount of backscatter is produced by the version of the model tested presently albeit not as much as is indicated by the filtered DNS field. An adjustable parameter in the model is the Kolmogorov constant. The value presently used is within the bounds of experimental values. The model is about 25% more expensive in CPU time than the simple Smagorinsky model. Some subgrid model features show qualitative but not strong quantitative agreement with the equivalent quantities from filtered DNS fields at a similar Reynolds number. It remains to be seen how well the model will function for free-shear or wall-bounded flows. Future work will aim at constructing models with alternative representations of the subgrid vortex orientations.

Acknowledgments

AM was partially supported under NSF Grant CTS-9634222 and wishes to acknowledge fruitful discussions with Prof. D. I. Pullin. Hospitality provided by CTR during the 1996 Summer Program is gratefully acknowledged.

REFERENCES

COMTE-BELLOT, G. & CORRSIN, S. 1971 Simple Eulerian time correlation of full and narrow-band velocity signals in grid-generated 'isotropic' turbulence. *J. Fluid Mech.* **48**, 273-337.

CARATI, D., GHOSAL, S. & MOIN, P. 1995 On the representation of backscatter in dynamic localization models. *Phys Fluids* **7**(3), 606-616.

JIMÉNEZ J., WRAY A., SAFFMAN, P. G. & ROGALLO, R. S. 1993 The structure of intense vorticity in homogeneous isotropic turbulence. *J. Fluid Mech.* **255**, 65-90.

LUNDGREN, T. S. 1982 Strained spiral vortex model for turbulent fine structure. *Phys Fluids* **25**, 2193-2203.

MASON, P. AND THOMSON, D. 1992 Stochastic backscatter in large-eddy simulation of boundary layers. *J. Fluid Mech.* **242**, 51-78.

MISRA, A. & PULLIN, D. I. 1996 A vortex-based subgrid stress model for large-eddy simulation. Submitted to *Phys Fluids*

PIOMELLI, U., CABOT, W. H., MOIN, P., LEE, S. 1991 Subgrid-scale backscatter in turbulent and transitional flows. *Phys Fluids* **8**, 215-224.

PIOMELLI, U., YU, Y. & ADRIAN, R. 1996 Subgrid-scale energy transfer and near-wall turbulence. *Phys Fluids* **8**, 215-224.

PULLIN, D. I. & SAFFMAN, P. G. 1993 On the Lundgren-Townsend model of turbulent fine scales, *Phys Fluids A* **5**, 126-145.

PULLIN, D. I. & SAFFMAN, P. G. 1994 Reynolds stresses and one-dimensional spectra for a vortex model of homogeneous anisotropic turbulence. *Phys Fluids* **6**, 3010-3027.

REYNOLDS, W. C. & KASSINOS, S. 1995 One-point modeling of rapidly deformed homogeneous turbulence. *Proc. R. Soc. London* **A**, 87-104.

SMAGORINSKY, J. 1963 General circulation experiments with primitive equations. *Mon. Weather Rev.* **91**, 99.

SREENIVASAN, K. R. 1995 On the universality of the Kolmogorov constant. *Phys Fluids* **7**(11), 2778-2784.

VINCENT, A. & MENEGUZZI, M. 1994 The dynamics of vorticity tubes in homogeneous turbulence. *J. Fluid Mech.* **258**, 245-254.